Two-Dimensional Mixed-Ligand Metal-Organic Framework Constructed from Bridging Bidentate V-Shaped Ligands

Wen-Wu Zhong, Fahimeh Dehghani Firuzaba, Younes Hanifehpour, Xue Zeng, Yuan-Jiao Feng, Kuan-Guan Liu, Sang Woo Joo, Ali Morsali, Pascal Retailleau

inorganics

MDPI

Article

Two-Dimensional Mixed-Ligand Metal–Organic Framework Constructed from Bridging Bidentate V-Shaped Ligands

Wen-Wu Zhong [1,2], Fahimeh Dehghani Firuzabadi [3], Younes Hanifehpour [4,*], Xue Zeng [1,2], Yuan-Jiao Feng [1,2], Kuan-Guan Liu [5], Sang Woo Joo [6,*], Ali Morsali [7,*] and Pascal Retailleau [8]

1 Chongqing Medical and Pharmaceutical College, No. 82 Middle College-City Road, Chongqing 401331, China; zhongww111@163.com (W.-W.Z.); zhenxue520@163.com (X.Z.); fengyuanj88@126.com (Y.-J.F.)
2 Chongqing Engineering Technology Research Center of Pharmaceutical Preparation, No. 82 Middle College-City Road, Chongqing 401331, China
3 Department of Chemistry, College of Sciences, Shiraz University, Shiraz 71454, Iran; dehghani7843@gmail.com
4 Department of Chemistry, Sayyed Jamaleddin Asadabadi University, Asadabad 6541861841, Iran
5 Key Laboratory of Ningxia for Photovoltaic Materials, Ningxia University, Yinchuan 750021, China; liukuanguan@nxu.edu.cn
6 School of Mechanical Engineering, Yeungnam University, Gyeongsan 712-749, Republic of Korea
7 Department of Chemistry, Faculty of Sciences, Tarbiat Modares University, Tehran P.O. Box 14115-175, Iran
8 Service de Cristallochimie, Université Paris-Saclay, Institut de Chimie des Substances Naturelles-CNRS, Bât 27, 1 Avenue de la Terrasse, 91190 Gif-sur-Yvette, France; pascal.retailleau@cnrs.fr
* Correspondence: younes.hanifehpour@gmail.com (Y.H.); swjoo@yu.ac.kr (S.W.J.); morsali_a@modares.ac.ir (A.M.)

Abstract: A two-dimensional and bifunctional pillar-layered metal–organic framework (MOF)—with the molecular formula [Zn(*cba*)(*bpdb*)]·DMF (**2DTMU-1**), H_2cba = 4,4′-methylenedibenzoic acid, bpdb = 1,4-bis(4-pyridyl)-2,3-diaza-1,3-butadiene—was obtained via the reaction of zinc(II) nitrate with H_2cba as the carboxylate linker and *bpdb* as the N-donor pillar. **2DTMU-1** is based on a binuclear paddlewheel Zn(II) unit complexed by four bridging bidentate (dicarboxylate) V-shaped ligands, which combine to from H_2cba; this tetragonal array, which is connected by *bpdb* with a bridging azine group, presents a pore size of 18 × 12 Å^2.

Keywords: metal–organic framework; ditopic carboxylate ligand; polymers; porous materials

Citation: Zhong, W.-W.; Dehghani Firuzabadi, F.; Hanifehpour, Y.; Zeng, X.; Feng, Y.-J.; Liu, K.-G.; Joo, S.W.; Morsali, A.; Retailleau, P. Two-Dimensional Mixed-Ligand Metal–Organic Framework Constructed from Bridging Bidentate V-Shaped Ligands. *Inorganics* **2023**, *11*, 184. https://doi.org/10.3390/inorganics11050184

Academic Editor: Francis Verpoort

Received: 10 February 2023
Revised: 10 April 2023
Accepted: 21 April 2023
Published: 25 April 2023

1. Introduction

Metal–organic frameworks (MOFs) are subclasses of coordination polymers, which are often porous and created via the careful selection of metal ions or metal clusters alongside connecting linkers formed via coordination bonds [1–6]. In addition to coordination bonds, there are non-covalent interactions that occur, such as hydrogen bonding, π–π stacking between aromatic groups, and Van der Waals forces, which produce superstructures, flexibility, and dynamic porous compounds. Hydrogen bonds provide structural resistance that prevents the filling of space and thus allows for the growth of open frameworks [7,8]. In the synthesis of MOFs with metal ions and organic linkers, the flexibility around the metal ion often leads to the lack of proper control and the production of multiple structures; thus, oxygen-donating groups such as carboxylates are used to chelate the metal ions, whose interlocking is also used, resulting in oriented metal–oxygen–carbon clusters, which form geometric shapes called secondary structural units (SBU) [9]. In many reports, carboxylate ligands are usually chosen for the synthesis of MOFs because they act as both counter ions and bridging ligands with which to expand one-, two-, and three-dimensional structures [10]. For the design of favorable MOFs, the nature of the ligand used is very important [11–13]. For example, the use of aromatic polycarboxylate ligands leads to the production of MOFs with suitable coordination modes and high structural stability [14]. In the design and synthesis of MOFs with many dimensions, ligands with oxygen and nitrogen donors are

often used [7,15–17]. The presence of different donor centers leads to the possibility of complexation due to linkage isomerism, and despite the difficulties of purification and identification experiments, this becomes a useful tool for the design of multi-dimensional MOFs. By employing various ligands or linkers, the preparation of special molecular frameworks with desirable properties can be realized. For example, through the use of N- and O-donor ligands (pyridine carboxylates), sensor compounds can be developed [18].

MOFs have been the focus of considerable attention due to their unique properties, such as their good crystallinity, high specific surface area, organic–inorganic hybrid nature, structural stability, and tunability in terms of pore size and structural features [19]. They are appealing for research due to their variety of properties and applications in chemistry and materials science [2,20–22]. The careful selection and rational architectural design of MOF structural units promotes their use in various applications, such as sensing [23], catalysis [24], drug delivery [25], and gas storage [26]. In particular, the functional groups of ligands have a significant influence on the chemical properties of MOFs. In addition, by controlling the dimensions and morphology of MOFs, it is possible to create more favorable physical and chemical properties for some advanced applications [27–31].

MOFs are often three-dimensional, although some two-dimensional MOFs have recently been developed [2,32]. In recent years, the construction of 2D MOFs has received a lot of attention owing to their fascinating structural features, such as their high surface area, high density of exposed functional sites, and capacity for more interactions between the substrate molecules and MOF surface, which are advantageous for various applications [33–35]. The 2D extended network can offer favorable performance in processes such as light harvesting and rapid electron and energy migration. Therefore, 2D MOFs have shown high applicatory potential in electronics, chemical sensing, catalysis, and gas separation [36,37].

Polytopic carboxylic ligands (linear or bent ditopic, tritopic, and tetratopic) are often used in the synthesis of MOFs, although angularly bent ligands ($0^\circ \leq \theta < 180^\circ$) are also applied for the synthesis of extended polyhedral structures [38]. On the other hand, pillared MOFs based on paddle-wheel nodes can be structurally classified into two different groups depending on the geometry and multitopic nature of the carboxylate linkers involved. In the first group, 2D metal–carboxylate layers are developed due to the coordination of deprotonated carboxylate groups to the metal ions and the formation of paddle-wheel inorganic nodes. In this regard, tetratopic planar [39] and linear ditopic [40] carboxylate linkers can form such 2D layers. Then, these 2D metal–carboxylate linkers can be connected through the coordination of N-donor pillars for the construction of 3D frameworks. In the second group, 1D metal–carboxylate chains can be constructed via the coordination of bent ditopic carboxylate linkers. In this work, we synthesized a two-dimensional Zn(II) metal–organic framework, [Zn(*cba*)(*bpdb*)]·DMF (**2DTMU-1**), based on a V-shaped flexible dicarboxylate ligand, 4,4′-methylenedibenzoic acid (H_2cba), and an N-donor ligand, 1,4-bis(4-pyridyl)-2,3-diaza-1,3-butadiene (*bpdb*). In addition, the effect of the-CH_2- group of H_2cba was compared with similar reported pillared MOFs, TMU-4, and TMU-5. The use of 4,4′-oxybis(benzoic acid) (H_2oba) as a linker was applied in the structures of TMU-4 and TMU-5 (Scheme 1).

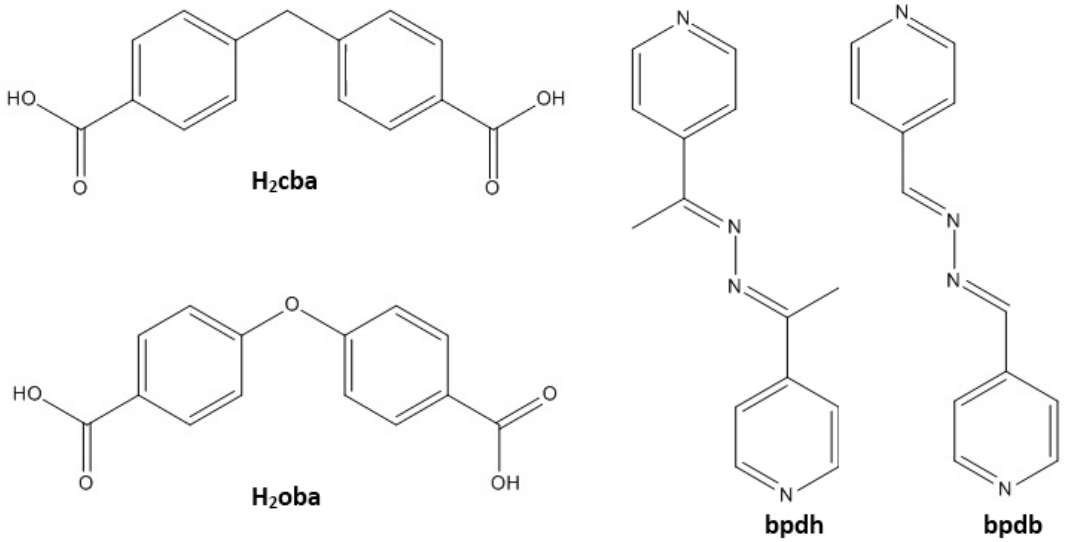

Scheme 1. Structural formulas of ditopic carboxylate linkers and nitrogen donor pillar ligand used in the structures of [Zn(*cba*)(*bpdb*)]·DMF (**2DTMU-1**), $[Zn_2(oba)_2(bpdb)]_n \cdot (DMF)_x$ (TMU-4), and $[Zn(oba)(bpdh)_{0.5}]_n \cdot (DMF)_y$ (TMU-5).

2. Results and Discussion

A new two-dimensional Zn(II) metal–organic framework, [Zn(*cba*)(*bpdb*)]·DMF (**2DTMU-1**), was synthesized by mixing zinc(II) nitrate with a V-shaped flexible dicarboxylate ligand, 4,4′-methylenedibenzoic acid (H_2cba), and an N-donor ligand, 1,4-bis(4-pyridyl)-2,3-diaza-1,3-butadiene (*bpdb*). The structure of this new MOF compound was determined via infrared spectroscopy and single-crystal X-ray crystallography. (IR data (KBr pellet, ν/cm^{-1}): selected bands—775 (s), 874 (m), 1088 (s), 1159 (s), 1242 (*v*s), 1413 (*v*s-br), 1503 (s), 1602 (*v*s), 1679 (*v*s), and 3418 (w-br).) The weak absorption band at 3418 cm^{-1} can be ascribed to the C–H vibration of the aromatic rings. The absorption bands at 1602, 1503, and 1413 cm^{-1} correspond to vibrations of the py ring of the ligands. The band at 1242 cm^{-1} is related to C–H vibration of the cba^{2-} portion. The absorption of the C=O vibration for DMF was observed at 1679 cm^{-1}. The single-crystal structural determination analysis indicated that the **2DTMU-1** framework is a pillar-layered framework based on ditopic bent cba^{2-} carboxylate linker and *bpdb* N-donor pillar. One-dimensional metal–carboxylate chains were constructed based on paddle-wheel inorganic nodes via the coordination of deprotonated H_2cba linkers to the Zn(II) metal ions (Figure 1). Then, these 1D chains were connected by a *bpdb* pillar spacer to form the 2D framework of **2DTMU-1** (Figure 2a). The inter-digited layers of **2DTMU-1** are presented in Figure 3b. The *bpdb* linkers bear an azine group; in fact, the 2D framework of **2DTMU-1** was functionalized with azine functional groups (Figure 2b). The large voids (ca. 18 × 12 $Å^2$) for each two-dimensional coordination polymer allow for parallel interpenetration to occur between the adjacent structures (Figure 3).

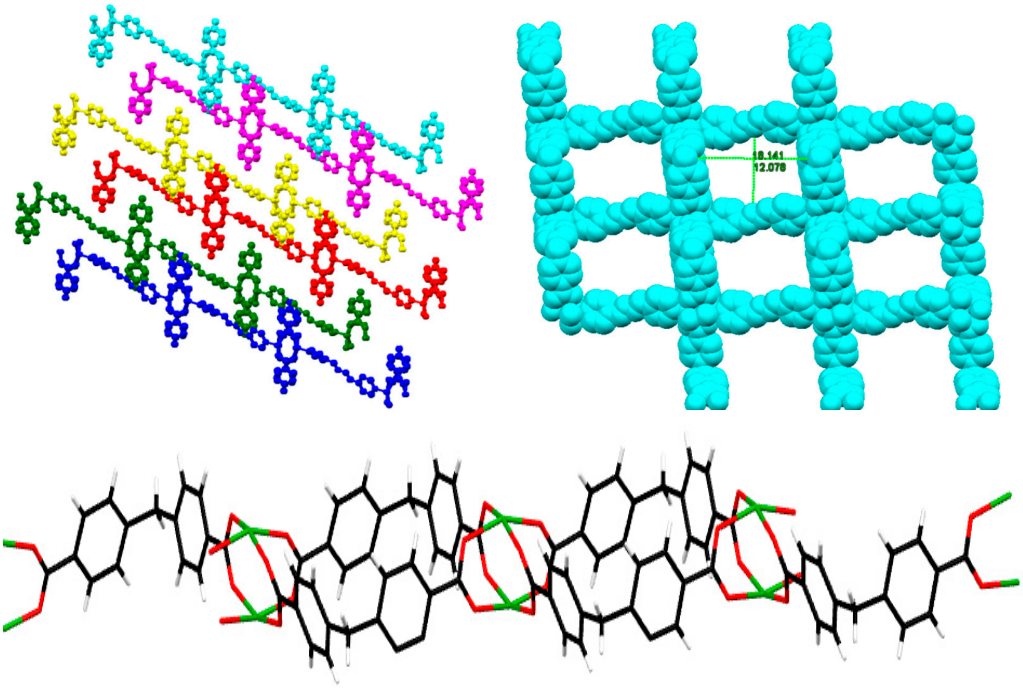

Figure 1. The representation of 1D chains of Zn-cba in **2DTMU-1** framework.

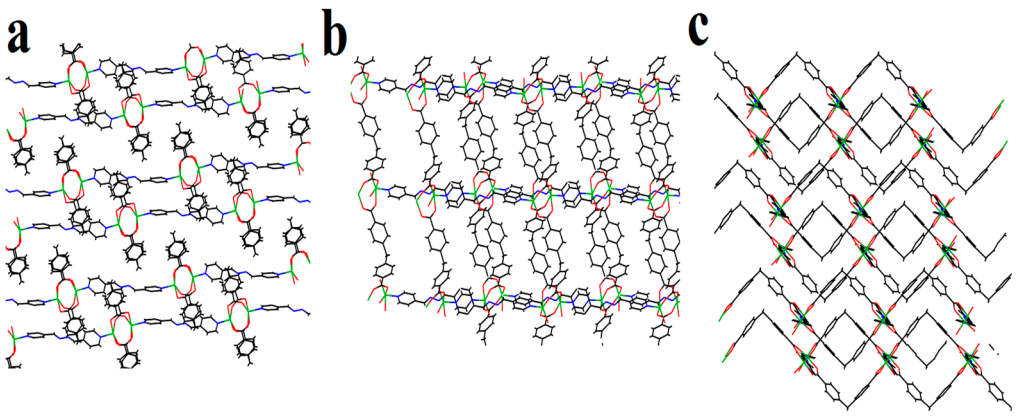

Figure 2. Schematic representation of 2D framework of **2DTMU-1**: (**a**) along the A axis; (**b**) along the B axis; (**c**) along the C axis.

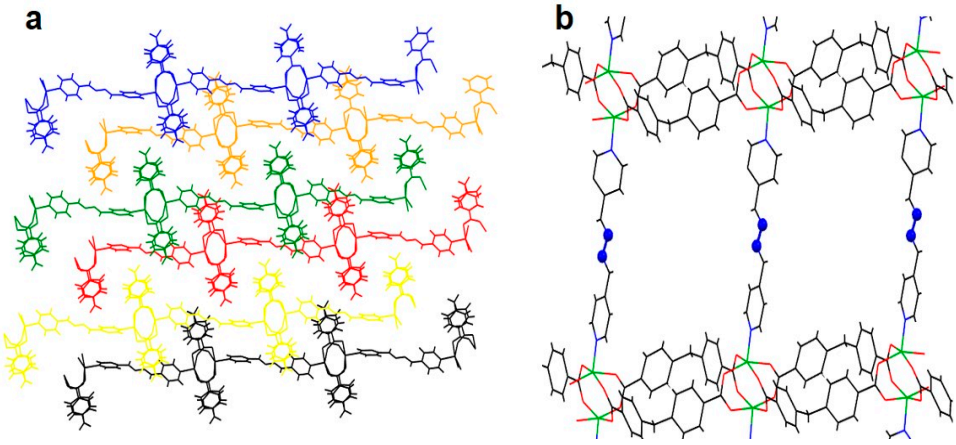

Figure 3. (**a**) Interdigitated layers and (**b**) azine-decorated framework of **2DTMU-1**.

2DTMU-1 has 2D (4,4) layered structure and crystallizes in the triclinic plane with the space group of *Pī*. The Zn(II) center is five-coordinated by four oxygen atoms from four cba^{2-} ligands and one nitrogen atom from one *bpdb* ligand, yielding a geometry with a distorted trigonal bipyramidal structure. The Zn–O and Zn–N bond lengths and O–Zn–O and O–Zn–N bond angles range from 2.032(3) to 2.051(3) Å and 87.74 (12) to 163.68(11)°, respectively, within the region of the values observed for similar Zn(II) complexes with five coordination structures and oxygen and nitrogen donor ligands [1–3]. In the crystal structure of **2DTMU-1**, the cba^{2-} ligands bridge the same mode to link four Zn(II) centers, whereas the *bpdb* acts as a *trans*-bidentate bridging ligand that links pairs of Zn atoms. In this manner, the binuclear Zn units are bridged into a linear chain via cba^{2-} anions with a Zn···Zn separation of 19.63 Å. The *bpdb* ligands also link the binuclear zinc(II) atoms to construct a linear structure with a Zn···Zn distance of 12.63 Å. The two kinds of parallel structures are perpendicularly intersected by the dinuclear zinc atoms, thereby generating a two-dimensional (4,4) network (Figure 4) when the dimer zinc atoms and the organic parts are considered as nodes and linkers, respectively. Each ring forms from four cba^{2-} ligands, two *bpdb* ligands, and two Zn(II) atoms.

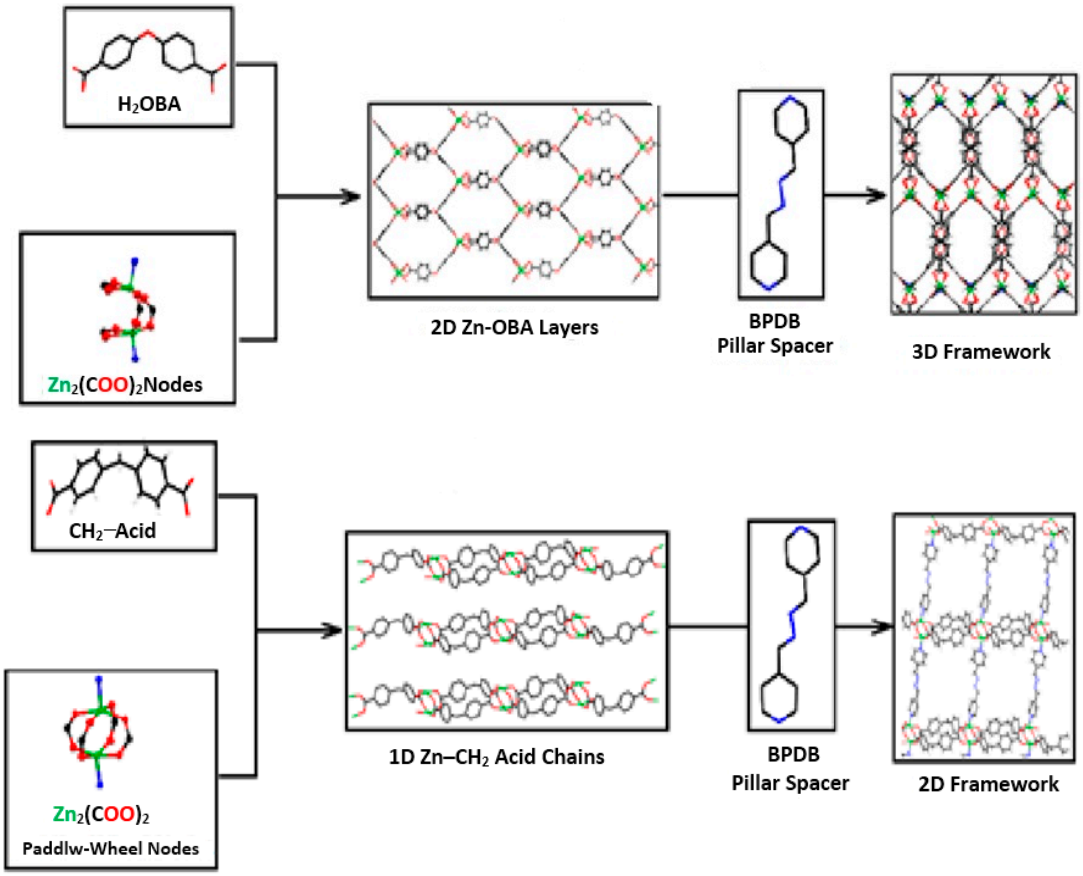

Figure 4. A schematic illustration of linkers and pillars used in TMU-4 (**up**) and **2DTMU-1** (**low**) with their 3D and 2D structures.

Two similar pillar-layered metal–organic frameworks have been reported [41], which incorporate a similar linker (H_2oba) and the same pillar ligands (*bpdb* and *bpdh*); azine-decorated TMU-4 with the formula $[Zn(oba)(bpdb)_{0.5}]_n \cdot 2DMF$; and azine–methyl-functionalized TMU-5 with the formula $[Zn(oba)(bpdh)_{0.5}]_n \cdot 1.5DMF$, where H_2oba = 4,4′-oxybis(benzoic acid), *bpdb* = 1,4-bis(4-pyridyl)-2,3-diaza-1,3-butadiene, and *bpdh* = 2,5-bis(4-pyridyl)-3,4-diaza-2,4-hexadiene. Figure 4 presents two different linkers, H_2oba and H_2cba, but the same bpdb pillared ligands were applied for the preparation of two structurally different MOFs, TMU-4 and **2DTMU-1**, along with their 3D and 2D structures.

As evident from their building blocks, *bpdb* is the pillar ligand in both compounds, and the ditopic carboxylate linkers are different, namely, H_2oba and H_2cba in TMU-4 and **2DTMU-1**, respectively. The main parts of the two linkers are the same, and the only difference is in the middle spacer part of these linkers; in H_2oba, the -O- groups were replaced with the -CH_2- group in H_2cba. This replacement influenced the type of structures grown in a three-dimensional manner, as can be seen in the structure of **2DTMU-1**. Bridging the cba^{2-} linkers to the paddle-wheel zinc-acetate-type nodes creates one-dimensional chains (Figure 5), which then connect through N-donor *bpdb* pillars and form 2D frameworks; however, in the case of TMU-4, the oba^{2-} linkers are bridged to the paddle-wheel zinc-acetate-type nodes, creating sheet-like, two-dimensional metal–carboxylate linkers, which can then be connected by the N-donor *bpdb* pillar to form 3D frameworks.

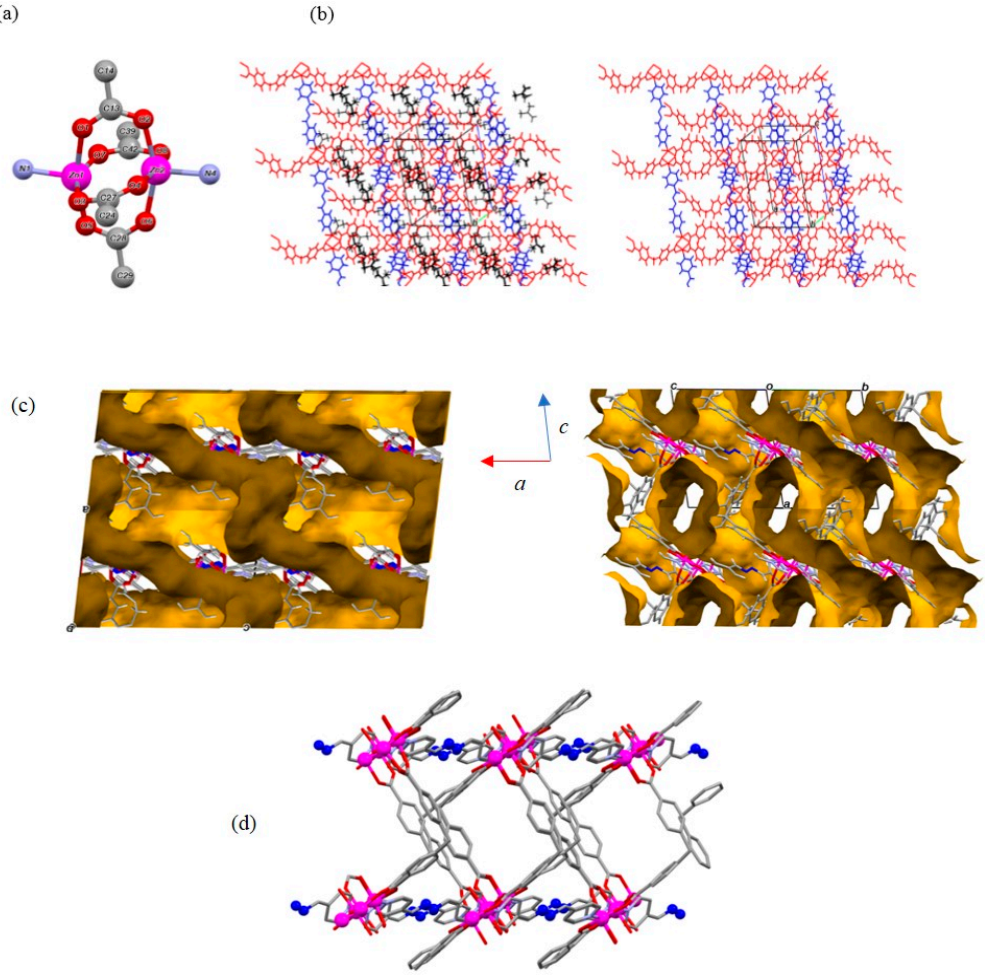

Figure 5. (**a**) Representation of the Zn2 paddlewheel unit within **2DTMU-1**. (**b**) Layers of Zn(II)-cba (in red) pillared with *bpdb* (in blue) along the *c* direction in the presence (**left**) or absence of solvent (**right**). (**c**) Connolly surface representation along *b*-axis (**left**) and *bc* direction (**right**), showing that **2DTMU-1** is porous and comprises interconnected pores. (**d**) Representation of the pores, highlighting the azine groups (in sea blue). Color code: O—red; N—blue; C—gray; and Zn—magenta. Connolly surface: gold represents the outside of the surface, and dark gold represents the inside of the surface.

However, **2DTMU-1** is formed on a binuclear paddlewheel Zn(II) unit (Zn**#** 1 and Zn**#** 2) complexed by four bridging bidentate (dicarboxylate) V-shaped ligand, 4,4′-methylenedibenzoic acid (H_2cba); this tetragonal array is connected by *bpdb* with an azine group bridging in the middle as a potential Lewis basic site. This assembly is similar to that obtained for

a TMU-5 [18] complex, in which both ligands had been replaced (H_2cba by H_2oba and *bpdb* by *bpdbh*, respectively) and not with TMU-4, which simply differs by one atom in the V-shaped ligand (O replaced by C, Figure 5). Nonetheless, **2DTMU-1** crystallizes in the centrosymmetric triclinic space group conversely to TMU-5 in a higher-symmetry space group (*C2/c*) as a consequence of the larger distortion of the paddlewheel unit. In fact, the square pyramidal geometry around the Zn centers is coordinated by four carboxylate O atoms (for Zn# 1: O1, O3, O5, and O7; for Zn# 2: O2, O4, O6, and O8) from four fully deprotonated cba^{2-} ligands with the bite-averaged angle of 125.4° and one N atom (Zn# 1: N1 and Zn# 2: N4 from the *bpdb* ligand in the axial direction appear to be particularly deformed, with a Zn#1–O distance ranging from 2.040(3) to 2.056(2) Å, respectively; for Zn#2: from 2.033(3) to 2.098(2) Å), but with similar Zn–N distances of 2.0412(3) Å (Figure 3). The averaged r.m.s.d of the atoms in the equatorial planes delineated by orienting the carboxylates at 89.5° with respect to each other is 0.125 Å. The separation between Zn# 1 and Zn# 2 is 2.934(1) Å, which is the same order of magnitude as that in TMU-5. The bond lengths and bond angles of **2DTMU-1** are listed in Table 1.

Table 1. Selected bond lengths (Å) and angles (°) for **2DTMU-1**.

Zn(1)-O(5)	2.040(2)	O(5)-Zn(1)-N(1)	99.68(9)
Zn(1)-N(1)	2.041(2)	O(5)-Zn(1)-O(3) $^{\#1}$	87.60(9)
Zn(1)-O(3) $^{\#1}$	2.047(2)	N(1)-Zn(1)-O(3) $^{\#1}$	110.72(10)
Zn(1)-O(1) $^{\#2}$	2.052(2)	O(5)-Zn(1)-O(1) $^{\#2}$	163.74(8)
Zn(1)-O(7) $^{\#3}$	2.056(2)	N(1)-Zn(1)-O(1) $^{\#2}$	96.35(9)
Zn(1)-Zn(2) $^{\#2}$	2.9338(5)	O(3) $^{\#1}$-Zn(1)-O(1) $^{\#2}$	89.28(9)
Zn(2)-O(2)	2.033(2)	O(5)-Zn(1)-O(7) $^{\#3}$	88.22(9)
Zn(2)-N(4)	2.042(2)	N(1)-Zn(1)-O(7) $^{\#3}$	94.92(10)
Zn(2)-O(6) $^{\#4}$	2.048(2)	O(3) $^{\#1}$-Zn(1)-O(7) $^{\#3}$	154.36(8)
Zn(2)-O(8) $^{\#5}$	2.050(2)	O(1) $^{\#2}$-Zn(1)-O(7) $^{\#3}$	87.71(9)
Zn(2)-O(4) $^{\#6}$	2.098(2)	O(5)-Zn(1)-Zn(2) $^{\#2}$	86.65(6)
		N(1)-Zn(1)-Zn(2) $^{\#2}$	162.94(8)
		O(3) $^{\#1}$-Zn(1)-Zn(2) $^{\#2}$	85.21(6)
		O(1) $^{\#2}$-Zn(1)-Zn(2) $^{\#2}$	77.19(6)
		O(7) $^{\#3}$-Zn(1)-Zn(2) $^{\#2}$	69.30(6)
		O(2)-Zn(2)-N(4)	102.58(9)
		O(2)-Zn(2)-O(6) $^{\#4}$	155.79(8)
		N(4)-Zn(2)-O(6) $^{\#4}$	100.92(9)
		O(2)-Zn(2)-O(8) $^{\#5}$	88.07(9)
		N(4)-Zn(2)-O(8) $^{\#5}$	103.56(9)
		O(6) $^{\#4}$-Zn(2)-O(8) $^{\#5}$	92.06(9)
		O(2)-Zn(2)-O(4) $^{\#6}$	87.52(9)
		N(4)-Zn(2)-O(4) $^{\#6}$	91.10(9)
		O(6) $^{\#4}$-Zn(2)-O(4) $^{\#6}$	86.28(9)
		O(8) $^{\#5}$-Zn(2)-O(4) $^{\#6}$	165.29(8)
		O(2)-Zn(2)-Zn(1) $^{\#4}$	82.66(6)
		N(4)-Zn(2)-Zn(1) $^{\#4}$	164.91(8)
		O(6) $^{\#4}$-Zn(2)-Zn(1) $^{\#4}$	73.13(6)
		O(8) $^{\#5}$-Zn(2)-Zn(1) $^{\#4}$	90.66(6)
		O(4) $^{\#6}$-Zn(2)-Zn(1) $^{\#4}$	74.87(6)

Symmetry transformations used to generate equivalent atoms: $^{\#1}$ x+1, y, z+1. $^{\#2}$ x, y, z+1. $^{\#3}$ x−1, y, z. $^{\#4}$ x, y, z−1. $^{\#5}$ x−1, y, z−1. $^{\#6}$ x+1, y, z.

3. Experimental Section

3.1. Materials and Physical Measurements

All the starting materials and solvents for the preparation and spectroscopic analysis were purchased from Aldrich and Merck and used as received. Melting points were measured using an Electrothermal 9100 apparatus. Infrared spectra were recorded using Thermo Nicolet IR 100 FT-IR. For X-ray crystal structure determination, one of the approximately spherical habits was measured at 100 K under liquid nitrogen stream using a

RIGAKU *XtaLabPro* diffractometer equipped with a Mo microfocus sealed-tube *MM003* generator coupled to a double-bounce confocal Max-Flux® multilayer optical device and an HPAD *PILATUS3R 200K* detector. *CrysAlisPro 1.171.41.123a* [42], incorporating a combination of spherical and empirical absorption corrections (using equivalent radius and absorption coefficients on the one hand and spherical harmonics on the other) into the *SCALE3 ABSPACK* scaling algorithm, was used for data processing and to deal with icing problems during data collection. The structure was determined via intrinsic phasing methods (*SHELXT* program) [43]; then, full-matrix least-squares methods with respect to F^2 using *SHELX-L* were applied for refinement [43]. All non-hydrogen atoms were improved by anisotropic refinement. Aromatic H atoms were placed in idealized positions and constrained to remain on their parent atoms with relative isotropic displacement coefficients, $U_{iso}(H)$, set to $1.2U_{eq}(C)$.

3.2. Synthesis of the Ligand and MOF

The ligand *bpdb* (1,4-bis(4-pyridyl)-2,3-diaza-1,3-butadiene) was synthesized via the method reported in [44]. Suitable crystals for single-crystal X-ray diffraction (*SCXRD*) analysis of **2DTMU-1** were prepared via the reaction of $Zn(NO_3)_2{\cdot}6H_2O$ (0.297 g, 1 mmol), 4,4′-methylenedibenzoic acid (H_2cba) (0.254 g, 1 mmol) and 1,4-bis(4-pyridyl)-2,3-diaza-1,3-butadiene (*bpdb*) (0.105 g, 0.5 mmol) in 30 mL of DMF. This reaction mixture was sonicated for uniform dispersion (∼3 min) followed by heating at 80 °C. After 72 h, the yellow **2DTMU-1** crystals were collected (0.420 g; yield—71% based on H_2cba), for which d.p. > 300 °C. IR data (KBr pellet, ν/cm^{-1}): selected bands—775 (s), 874 (m), 1088 (s), 1159 (s), 1242 (*v*s), 1413 (*v*s-br), 1503 (s), 1602 (*v*s), 1679 (*v*s), and 3418 (w-br), as shown in Figure 6. The crystals of **2DTMU-1** were heated at 100 °C for 8 h to obtain the de-solvated or activated product. IR spectra for the activated product showed that the band at 1679 cm^{-1} related to DMF solvent had disappeared.

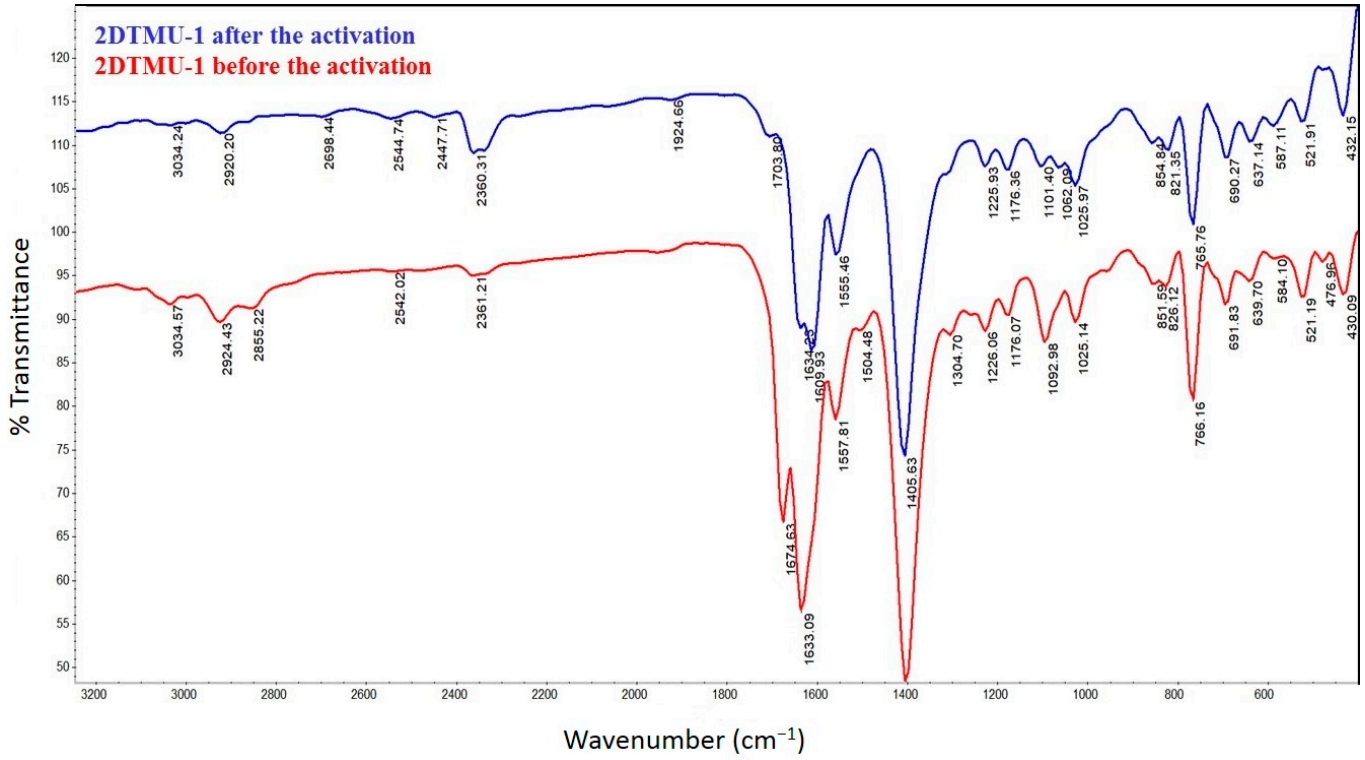

Figure 6. IR spectra of the **2DTMU-1** before and after the activation process.

3.3. Determination of the Crystal Structure of 2DTMU-1

The structure of **2DTMU-1** contains 1100 $Å^3$ (*ca* 41% of the unit-cell volume) of solvent-accessible voids, which were revealed using the *SQUEEZE* routine [45] as implemented in the program *PLATON* (Spek, 2020), and is occupied by an estimated 267 electrons corresponding to *ca* 6.7 solvent molecules of DMF. Nevertheless, four DMF molecules could be modelled inside these cavities, among which were two DMFs with static disorder constrained by SHELXL instructions *(SADI*, *DELU*, *SIMU*, and *EADP)*. Methyl hydrogens were treated as rigid groups allowed to rotate but not tip with U_{iso}(H) set to 1.5U_{eq}(C). Crystal data, data collection, and details of structures' refinement are summarized in Table 2. CCDC 2153128 contains the supplementary crystallographic data for this paper (See Data Availability Statement). These data can be obtained free of charge from the Cambridge Crystallographic Data Centre at www.ccdc.cam.ac.uk.

Table 2. Crystal data and structural refinement for **2DTMU-1**.

Identification Code	**2DTMU-1 [Zn2(*cba*)2(*bpdb*)]·(DMF)y**
Empirical formula	C_{42} H_{30} N_4 O_8 Zn_2, 4 (C_3 H_7 N O)
Formula weight	1141.82
Temperature	100(2) K
Wavelength	0.71073 Å
Crystal system	Triclinic
Space group	P-1
Unit cell dimensions	a = 12.6848(9) Å, α = 78.658(5)° b = 12.9028(8) Å, β = 80.243(5)° c = 18.1796(9) Å, γ = 72.620(6)°
Volume	2764.6(3) $Å^3$
Z	2
Density (calculated)	1.382 Mg/m^3
Absorption coefficient	0.942 mm^{-1}
F(000)	1188
Crystal size	0.12 mm × 0.11 mm × 0.07 mm
θ range for data collection	2.550 to 25.349°
Index ranges	$-15 \leq h \leq 15$, $-15 \leq k \leq 14$, $-21 \leq l \leq 21$
Reflections collected	40891
Independent reflections	10063 [R(int) = 0.1061]
Completeness to θ = 25.242 Å	99.2%
Absorption correction	Sphere r 0.1 Å T 0.872
Refinement method	Full-matrix least-squares on F^2
Data/restraints/parameters	10,060/401/764
Goodness-of-fit for F^2	0.966
Final R indices [$I > 2\sigma(I)$]	R1 = 0.0452, wR2 = 0.0896
R indices (all data)	R1 = 0.0801, wR2 = 0.1003
Largest diff. peak and hole	0.444 and −0.472 e. $Å^{-3}$

4. Conclusions

A new bifunctional two-dimensional MOF and layered structure with the molecular formula [Zn(*cba*)(*bpdb*)]·DMF (2DTMU-1), incorporating 4,4′-methylenedibenzoic acid (H_2*cba*) as a carboxylate linker and 1,4-bis(4-pyridyl)-2,3-diaza-1,3-butadiene (*bpdb*) as a N-donor ligand, was synthesized and characterized. 2DTMU-1 was formed on a binuclear paddlewheel Zn(II) unit complexed by a four bridging bidentate (dicarboxylate) V-shaped ligand (H_2*cba*); this tetragonal array is connected by *bpdb* with an azine group bridging in the middle as a potential Lewis basic site. The synthesized MOF with a potential Lewis basic site presents a pore size of 18 × 12 $Å^2$. The results indicated that a small change in the nature of the ligands affected the structure and dimensions of the resulting MOFs. Thus, the use of two different carboxylate ligands with similar structures and the same pillar ligands led to the production of two MOFs with different structures and dimensions (one-dimensional and two-dimensional).

Author Contributions: W.-W.Z.: supervision, writing—review and editing; F.D.F.: writing—original draft preparation; Y.H.: supervision, writing—review and editing; X.Z.: draft preparation; Y.-J.F.: draft preparation; K.-G.L.: formal analysis; S.W.J.: project administration and editing; A.M.: supervision, writing—review and editing; P.R.: formal analysis. All authors have read and agreed to the published version of the manuscript.

Funding: We acknowledge the Scientific Research Project of Chongqing Medical and Pharmaceutical College (ygz2018303 and ygz2020112), the Natural Science Foundation of Chongqing Education Commission (kjqn282002802), and the Natural Science Foundation of Chongqing Science and Technology Commission (Cstc2020joyj-msxmx0194). This work was funded by grant NRF-2019R1A5A8080290 of the National Research Foundation of Korea.

Institutional Review Board Statement: Not applicable.

Informed Consent Statement: Not applicable.

Data Availability Statement: The supplementary crystallographic data were deposited on the Cambridge Crystallographic Data Centre (CCDC) as entry CCDC: 2153128.

Conflicts of Interest: The authors declare no conflict of interest.

References

1. Sanati, S.; Abazari, R.; Albero, J.; Morsali, A.; García, H.; Liang, Z.; Zou, R. Metal–organic framework derived bimetallic materials for electrochemical energy storage. *Angew. Chem. Int. Ed.* **2021**, *60*, 11048–11067. [CrossRef] [PubMed]
2. Masoomi, M.Y.; Morsali, A.; Dhakshinamoorthy, A.; Garcia, H. Mixed-MOFs: Unique opportunities in metal–organic framework (MOF) functionality and design. *Angew. Chem.* **2019**, *131*, 15330–15347. [CrossRef]
3. Liu, K.-G.; Sharifzadeh, Z.; Rouhani, F.; Ghorbanloo, M.; Morsali, A. Metal-organic framework composites as green/sustainable catalysts. *Coord. Chem. Rev.* **2021**, *436*, 213827. [CrossRef]
4. Razavi, S.A.A.; Masoomi, M.Y.; Morsali, A. Morphology-dependent sensing performance of dihydro-tetrazine functionalized MOF toward Al (III). *Ultrason. Sonochem.* **2018**, *41*, 17–26. [CrossRef]
5. Morsali, A.; Mahjoub, A. Coordination polymers of lead(II) with 4,4′-bipyridine: Syntheses and structures. *Polyhedron* **2004**, *23*, 2427–2436. [CrossRef]
6. Fard-Jahromi, M.J.S.; Morsali, A. Sonochemical synthesis of nanoscale mixed-ligands lead (II) coordination polymers as precursors for preparation of $Pb_2(SO_4)O$ and PbO nanoparticles; thermal, structural and X-ray powder diffraction studies. *Ultrason. Sonochem.* **2010**, *17*, 435–440. [CrossRef]
7. Beobide, G.; Castillo, O.; Cepeda, J.; Luque, A.; Pérez-Yáñez, S.; Román, P.; Thomas-Gipson, J. Metal–carboxylato–nucleobase systems: From supramolecular assemblies to 3D porous materials. *Coord. Chem. Rev.* **2013**, *257*, 2716–2736. [CrossRef]
8. Farrusseng, D. *Metal-Organic Frameworks: Applications from Catalysis to Gas Storage*; John Wiley & Sons: Hoboken, NJ, USA, 2011.
9. OYaghi, M.; O'Keeffe, M.; Ockwig, N.W.; Chae, H.K.; Eddaoudi, M.; Kim, J. Reticular synthesis and the design of new materials. *Nature* **2003**, *423*, 705–714. [CrossRef]
10. Thakuria, H.; Das, G. CuO micro plates from a 3D metallo-organic framework (MOF) of a binary copper (II) complex of *N*,*N*-bis(2-hydroxyethyl) glycine. *Polyhedron* **2007**, *26*, 149–153. [CrossRef]
11. Bigdeli, F.; Morsali, A.; Retailleau, P. Syntheses and characterization of different zinc (II) oxide nano-structures from direct thermal decomposition of 1D coordination polymers. *Polyhedron* **2010**, *29*, 801–806. [CrossRef]
12. Safarifard, V.; Rodríguez-Hermida, S.; Guillerm, V.; Imaz, I.; Bigdeli, M.; Tehrani, A.A.; Juanhuix, J.; Morsali, A.; Casco, M.E.; Silvestre-Albero, J. Influence of the amide groups in the CO_2/N_2 selectivity of a series of isoreticular, interpenetrated metal–organic frameworks. *Cryst. Growth Des.* **2016**, *16*, 6016–6023. [CrossRef]
13. Sadeghzadeh, H.; Morsali, A. Hedge balls nano-structure of a mixed-ligand lead (II) coordination polymer; thermal, structural and X-ray powder diffraction studies. *Cryst. Eng. Comm.* **2010**, *12*, 370–372. [CrossRef]
14. Lin, H.-Y.; Mu, B.; Wang, X.-L.; Tian, A.-X. Three copper (II) complexes connected through tetradentate carboxylate linkers and bidentate N-heterocyclic ligands: From 3-D MOF to 1-D chain. *J. Organomet. Chem.* **2012**, *702*, 36–44. [CrossRef]
15. Hashemi, L.; Morsali, A. Microwave assisted synthesis of a new lead (II) porous three-dimensional coordination polymer: Study of nanostructured size effect on high iodide adsorption affinity. *Cryst. Eng. Comm.* **2012**, *14*, 779–781. [CrossRef]
16. Masoomi, M.Y.; Morsali, A.; Junk, P.C. Ultrasound assisted synthesis of a Zn (II) metal–organic framework with nano-plate morphology using non-linear dicarboxylate and linear N-donor ligands. *RSC Adv.* **2014**, *4*, 47894–47898. [CrossRef]
17. Ranjbar, Z.R.; Morsali, A. Sonochemical syntheses of a new nano-sized porous lead (II) coordination polymer as precursor for preparation of lead (II) oxide nanoparticles. *J. Mol. Struct.* **2009**, *936*, 206–212. [CrossRef]
18. Teo, P.; Hor, T.A. Spacer directed metallo-supramolecular assemblies of pyridine carboxylates. *Coord. Chem. Rev.* **2011**, *255*, 273–289. [CrossRef]
19. Razavi, S.A.A.; Morsali, A.; Piroozzadeh, M. A Dihydrotetrazine-Functionalized Metal–Organic Framework as a Highly Selective Luminescent Host–Guest Sensor for Detection of 2,4,6-Trinitrophenol. *Inorg. Chem.* **2022**, *61*, 7820–7834. [CrossRef]

20. Kreno, L.E.; Leong, K.; Farha, O.K.; Allendorf, M.; Van Duyne, R.P.; Hupp, J.T. Metal–organic framework materials as chemical sensors. *Chem. Rev.* **2012**, *112*, 1105–1125. [CrossRef]
21. Furukawa, H.; Ko, N.; Go, Y.B.; Aratani, N.; Choi, S.B.; Choi, E.; Yazaydin, A.Ö.; Snurr, R.Q.; O'Keeffe, M.; Kim, J. Ultrahigh porosity in metal-organic frameworks. *Science* **2010**, *329*, 424–428. [CrossRef]
22. Rouhani, F.; Morsali, A. Fast and Selective Heavy Metal Removal by a Novel Metal-Organic Framework Designed with In-Situ Ligand Building Block Fabrication Bearing Free Nitrogen. *Chem. Eur. J.* **2018**, *24*, 5529–5537. [CrossRef]
23. Hu, M.-L.; Razavi, S.A.A.; Piroozzadeh, M.; Morsali, A. Sensing organic analytes by metal–organic frameworks: A new way of considering the topic. *Inorg. Chem. Front.* **2020**, *7*, 1598–1632. [CrossRef]
24. Bigdeli, F.; Abedi, S.; Hosseini-Monfared, H.; Morsali, A. An investigation of the catalytic activity in a series of isoreticular Zn (II)-based metal-organic frameworks. *Inorg. Chem. Commun.* **2016**, *72*, 122–127. [CrossRef]
25. Motakef-Kazemi, N.; Shojaosadati, S.A.; Morsali, A. In situ synthesis of a drug-loaded MOF at room temperature. *Microporous Mesoporous Mater.* **2014**, *186*, 73–79. [CrossRef]
26. Akhbari, K.; Morsali, A. Modulating methane storage in anionic nano-porous MOF materials via post-synthetic cation exchange process. *Dalton Trans.* **2013**, *42*, 4786–4789. [CrossRef] [PubMed]
27. Afshariazar, F.; Morsali, A. A dual-response regenerable luminescent 2D-MOF for nitroaromatic sensing via target-modulation of active interaction sites. *J. Mater. Chem. C* **2021**, *9*, 12849–12858. [CrossRef]
28. Parsa, F.; Ghorbanloo, M.; Morsali, A.; Wang, J.; Junk, P.C.; Retailleau, P. Azobenzene based 2D-MOF for high selective quinone fluorescence sensing performance. *Inorg. Chim. Acta* **2020**, *510*, 119699. [CrossRef]
29. Chakraborty, G.; Park, I.-H.; Medishetty, R.; Vittal, J.J. Two-dimensional metal-organic framework materials: Synthesis, structures, properties and applications. *Chem. Rev.* **2021**, *121*, 3751–3891. [CrossRef]
30. Abdollahi, N.; Masoomi, M.Y.; Morsali, A.; Junk, P.C.; Wang, J. Sonochemical synthesis and structural characterization of a new Zn (II) nanoplate metal–organic framework with removal efficiency of Sudan red and Congo red. *Ultrason. Sonochem.* **2018**, *45*, 50–56. [CrossRef]
31. Masoomi, M.Y.; Bagheri, M.; Morsali, A. Porosity and dye adsorption enhancement by ultrasonic synthesized Cd (II) based metal-organic framework. *Ultrason. Sonochem.* **2017**, *37*, 244–250. [CrossRef]
32. Zhang, X.; Xamena, F.L.I.; Corma, A. Gold (III)–metal organic framework bridges the gap between homogeneous and heterogeneous gold catalysts. *J. Catal.* **2009**, *265*, 155–160. [CrossRef]
33. Wang, M.; Dong, R.; Feng, X. Two-dimensional conjugated metal–organic frameworks (2D c-MOFs): Chemistry and function for MOFtronics. *Chem. Soc. Rev.* **2021**, *50*, 2764–2793. [CrossRef] [PubMed]
34. Sun, L.; Campbell, M.G.; Dincă, M. Electrically conductive porous metal–organic frameworks. *Angew. Chem. Int. Ed.* **2016**, *55*, 3566–3579. [CrossRef]
35. Afshariazar, F.; Morsali, A. Target-Architecture Engineering of a Novel Two-Dimensional Metal–Organic Framework for High Catalytic Performance. *Cryst. Growth Des.* **2019**, *19*, 4239–4245. [CrossRef]
36. Su, J.; He, W.; Li, X.-M.; Sun, L.; Wang, H.-Y.; Lan, Y.-Q.; Ding, M.; Zuo, J.-L. High electrical conductivity in a 2D MOF with intrinsic superprotonic conduction and interfacial pseudo-capacitance. *Matter* **2020**, *2*, 711–722. [CrossRef]
37. Li, J.; Song, S.; Meng, J.; Tan, L.; Liu, X.; Zheng, Y.; Li, Z.; Yeung, K.W.K.; Cui, Z.; Liang, Y. 2D MOF periodontitis photodynamic ion therapy. *J. Am. Chem. Soc.* **2021**, *143*, 15427–15439. [CrossRef]
38. Ahmad, N.; Younus, H.A.; Chughtai, A.H.; Van Hecke, K.; Khattak, Z.A.; Gaoke, Z.; Danish, M.; Verpoort, F. Synthesis of 2D MOF having potential for efficient dye adsorption and catalytic applications. *Catal. Sci. Technol.* **2018**, *8*, 4010–4017. [CrossRef]
39. Ghasempour, H.; Wang, K.-Y.; Powell, J.A.; ZareKarizi, F.; Lv, X.-L.; Morsali, A.; Zhou, H.-C. Metal–organic frameworks based on multicarboxylate linkers. *Coord. Chem. Rev.* **2021**, *426*, 213542. [CrossRef]
40. Furukawa, H.; Cordova, K.E.; O'Keeffe, M.; Yaghi, O.M. The chemistry and applications of metal-organic frameworks. *Science* **2013**, *341*, 1230444. [CrossRef]
41. Masoomi, M.Y.; Stylianou, K.C.; Morsali, A.; Retailleau, P.; Maspoch, D. Selective CO_2 capture in metal–organic frameworks with azine-functionalized pores generated by mechanosynthesis. *Cryst. Growth Des.* **2014**, *14*, 2092–2096. [CrossRef]
42. OD, R. *CrysAlis PRO*; Rigaku Oxford Diffraction: Oxfordshire, UK, 2015.
43. Sheldrick, G.M. Crystal structure refinement with SHELXL. *Acta Crystallogr. Sect. C Struct. Chem.* **2015**, *71*, 3–8. [CrossRef]
44. Ciurtin, D.M.; Dong, Y.-B.; Smith, M.D.; Barclay, T.; Loye, H.-C.Z. Two versatile *N*,*N*′-bipyridine-type ligands for preparing organic− inorganic coordination polymers: New cobalt-and nickel-containing framework materials. *Inorg. Chem.* **2001**, *40*, 2825–2834. [CrossRef]
45. Spek, A.L. checkCIF validation ALERTS: What they mean and how to respond. *Acta Crystallogr. Sect. E Crystallogr. Commun.* **2020**, *76*, 1–11. [CrossRef]